

Non-Fermi-liquid behavior in nearly ferromagnetic metallic SrIrO₃ single crystals

G. Cao¹, V. Durairaj¹, S. Chikara¹, L. E. DeLong¹, S. Parkin², and P. Schlottmann³

¹Department of Physics and Astronomy, University of Kentucky, Lexington, KY 40506

²Department of Chemistry, University of Kentucky, Lexington, KY 40506

³Physics Department, Florida State University, Tallahassee, FL 32306

We report transport and thermodynamic properties of single-crystal SrIrO₃ as a function of temperature T and applied magnetic field H . We find that SrIrO₃ is a non-Fermi-liquid metal near a ferromagnetic instability, as characterized by the following properties: (1) small ordered moment but no evidence for long-range order down to 1.7 K; (2) strongly enhanced magnetic susceptibility that diverges as $T^{-\gamma}$ at low temperatures with $1/2 < \gamma < 1$, depending on the applied field; (3) heat capacity $C(T,H) \sim -T \log T$ that is readily amplified by low applied fields; (4) a strikingly large Wilson ratio at $T < 4\text{K}$; and (5) a $T^{3/2}$ -dependence of electrical resistivity over the range $1.7 < T < 120\text{K}$. A phase diagram based on the data implies SrIrO₃ is a rare example of a stoichiometric oxide compound that exhibits non-Fermi-liquid behavior near a quantum critical point ($T = 0$ and $\mu_0 H = 0.23\text{ T}$).

PACS: 75.40.-s, 74.20.Mn, 74.25.Ha

The discoveries of exotic ground states (p-wave superconductivity, non-Fermi liquid (NFL)) [1, 2] in layered ruthenates have inspired extensive investigations on 4d and 5d materials. Typified by their extended 5d orbitals, it is commonly expected that iridates should be more metallic and less magnetic than their 3d, 4d and 4f counterparts, because of the broader 5d-bandwidth and the weaker exchange interaction U , so that $Ug(E_F) < 1$, where $g(E_F)$ is the density of states at the Fermi energy. However, in marked contrast to these expectations, most of the known iridates, such as layered BaIrO_3 [3-7] and $\text{Sr}_{n+1}\text{Ir}_n\text{O}_{3n+1}$ ($n = 1$ and 2) [8-14], are insulators exhibiting weak ferromagnetism [15]. On the other hand, the layered 4d ruthenate analogs (BaRuO_3 , Sr_2RuO_4 and $\text{Sr}_3\text{Ru}_2\text{O}_7$) are metallic or even superconducting. Although the layered iridates order at relatively high temperatures ($T_c = 175, 240,$ and 285 K for BaIrO_3 , Sr_2IrO_4 and $\text{Sr}_3\text{Ir}_2\text{O}_7$, respectively), they attain only a small fraction of the expected ordered moment ($\mu_{or} = 0.03, 0.14$ and $0.037 \mu_B/\text{Ir}$, respectively) [6, 12, 14]. The iridates exhibit strong phase transition signatures in magnetization but none of their T_c 's and resistivities are very sensitive to high magnetic fields [6, 12, 14]. Although a metallic state does not commonly occur in the iridates, the unusual circumstances almost guarantee that it will exhibit extraordinary properties when it does occur. In this paper, we report anomalous transport and thermodynamic properties of single-crystal SrIrO_3 , which we find is a NFL metal with a ferromagnetic instability extrapolated to zero-temperature at an applied magnetic field $\mu_0 H = 0.23$ T.

There are several examples of intriguing quantum phenomena occurring in itinerant-electron materials that are on the borderline between ferromagnetism and paramagnetism [16-18], e.g. p-wave superconductivity in Sr_2RuO_4 [1], superconductivity

and ferromagnetism in ZrZn_2 [19] and URhGe [20], a ferromagnetic quantum critical point (QCP) in MnSi under pressure [21], a metamagnetic transition with QCP end-point tuned by a magnetic field in $\text{Sr}_3\text{Ru}_2\text{O}_7$ [2], and QCP with anomalous ferromagnetism in $\text{Sr}_4\text{Ru}_3\text{O}_{10}$ [22]. In numerous Ce, Yb and U compounds similar phenomena associated with a QCP, but with *antiferromagnetic* spin-fluctuations have been found [24], leading to the breakdown of Fermi-liquid behavior, including a divergent specific heat [$C/T \sim -\log T$] and unusual power laws in resistivity ρ and magnetic susceptibility χ at low temperatures [24, 25]. The QCP can be tuned by “control parameters” such as composition, pressure, magnetic field, etc. [23-25]. To our knowledge SrIrO_3 is the first *stoichiometric* metallic 5d system with a nearby QCP that can be readily tuned with *very modest magnetic fields*; such a rare combination makes SrIrO_3 a unique and desirable model system for studies of quantum criticality both experimentally and theoretically.

It is now qualitatively understood that the extended 5d orbital significantly enhances crystalline electric field splittings causing a partial breakdown of Hund’s rule, leading to a low spin state, $S = 1/2$ for Ir^{4+} ($5d^5$) ions, and a *d-p* hybridization between the transition metal and the oxygen octahedron enclosing it. These interactions generate strong electron-lattice coupling that can alter and distort the metal-oxygen bond lengths and angles, lifting the degeneracies of 5d-orbitals and precipitating orbital ordering.

Single crystals were grown using flux techniques described elsewhere [7]. The crystal structure was determined from a small fragment ($0.05 \times 0.05 \times 0.05 \text{ mm}^3$) using $\text{Mo } K\alpha$ radiation and a Nonius Kappa CCD single-crystal diffractometer. Heat capacity measurements were performed with a Quantum Design PPMS that utilizes a thermal-relaxation calorimeter operating in fields up to 9 T. Magnetic and transport properties

were measured using a Quantum Design MPMS 7T LX SQUID Magnetometer equipped with a Linear Research Model 700 AC bridge for transport measurements. We define the susceptibility as $\chi \equiv M/H$ in terms of the DC magnetization $M(T,H)$.

The crystal structure of SrIrO_3 is a monoclinic distortion of the hexagonal BaTiO_3 or 6H structure [26] with space group $C2/c$ (No.15) having lattice parameters $a = 5.604 \text{ \AA}$, $b = 9.618 \text{ \AA}$, $c = 14.170 \text{ \AA}$ and $\beta = 93.26^\circ$. It features a distorted six-layer hexagonal structure that consists of close-packed Sr-O layers stacked perpendicular to the c-axis in the sequence hcchcc, where h and c refer to hexagonal and cubic stacking. Ir-O octahedra share common corners across a c-layer and common faces across an h-layer, forming pairs of face-shared octahedra that are joined by common corners to a plane of corner-sharing octahedra.

Fig. 1a shows the DC magnetic susceptibility χ as a function of T at $\mu_0 H = 0.5 \text{ T}$ for $\mathbf{H} \parallel \mathbf{c}$ -axis (χ_c) and $\mathbf{H} \perp \mathbf{c}$ -axis (χ_{ab}). Both χ_c and χ_{ab} are clearly temperature-dependent and large, particularly for $T < 15 \text{ K}$. In contrast, IrO_2 is a Pauli paramagnet with χ ($\sim 10^{-4} \text{ emu/mole-Ir}$), i.e. χ is temperature-independent and much smaller than that of SrIrO_3 ($> 10^{-3} \text{ emu/mole-Ir}$). While the large values of χ_c and χ_{ab} for SrIrO_3 are most likely the consequence of a significant exchange enhancement, $Ug(E_F)$, the sharp rise below 15 K suggests the proximity to a ferromagnetic instability. (Note that χ_c surpasses χ_{ab} at $T < 5 \text{ K}$.) Indeed, the isothermal magnetization M at $T = 1.7 \text{ K}$ is already saturated at $\mu_0 H \sim 3 \text{ T}$, as seen in the inset to Fig. 1a. On the other hand, the corresponding ordered moment μ_{or} is less than 3% of that expected ($1 \mu_B/\text{Ir}$) for an $S = 1/2$ system and decreases with increasing T , which is indicative of a nearby Stoner instability.

The reciprocal susceptibilities χ_c^{-1} and χ_{ab}^{-1} display linear T -dependences, consistent with a Curie-Weiss behavior for $T > 120$ K, as shown in Fig.1b. However, the Curie-Weiss fits of the data yield effective moments and Curie-Weiss temperatures that are much too large to be physically meaningful. This behavior is similar to the observed for the exchange-enhanced paramagnet SrRhO₃ [27, 28] and the metallic weak-ferromagnets ZrZn₂ [29] and Sc₃In [30]. Moreover, for $1.7 < T < 15$ K, χ_c^{-1} and χ_{ab}^{-1} follow non-standard power laws that range from $T^{1/2}$ for $B < 0.3$ T to linear- T for $B > 0.8$ T, as shown in Fig. 1c. This high sensitivity of the temperature exponent to low applied magnetic fields again suggests the rapid approach to a ferromagnetic instability.

The low temperature specific heat $C(T,H)$ data acquired over $1.8 < T < 24$ K and $\mu_0 H < 8$ T offer important insights into the low energy excitations of SrIrO₃. For $T > 12$ K, the specific heat is well described by $C(T) = \gamma T + \beta T^3$ with $\gamma = 1.50$ mJ/mole K² and $\beta = 0.28$ mJ/mole K⁴, suggesting that only electronic and phonon contributions are significant in this temperature range (data not shown). The small γ -value implies that there is essentially no mass enhancement and from the β -value we obtain a Debye temperature of 326 K.

The heat capacity data exhibit intriguing temperature and field dependences below 13 K, as shown in Fig.2a, where C/T vs T is plotted for $1.8 < T < 12.8$ K. A broad shoulder is observed near 4.5 K, which weakens with increasing field and eventually vanishes at $\mu_0 H > 3$ T. The field dependence suggests a magnetic mechanism, but $\chi(T,H)$ shows no corresponding transition. This broad peak in C/T is followed at lower temperatures by a pronounced $\log(T)$ dependence, characteristic of NFL systems [19], and suggests a vanishing Fermi temperature ($T_F \rightarrow 0$) and a divergent quasi-particle

effective mass ($m^*/m \rightarrow \infty$). It is clear that the amplitude of the logarithmic term rapidly grows with increasing field until $\mu_0 H = 1.1$ T, where it becomes weaker, and eventually vanishes for $\mu_0 H > 2$ T. Noticeably, C/T below 6 K is essentially constant for $\mu_0 H = 3$ T and then slowly drops off with decreasing T and increasing H , which indicates the removal of magnetic entropy and the recovery of Fermi-liquid behavior. This crossover is illustrated in Fig. 2a, which also presents a plot of C vs $T^{3/2}$ (right and upper scales) at $\mu_0 H = 8$ T. Hence, due to a magnetic field of 8 T, $C(T,H)$ evolves from the NFL $T \log(T)$ behavior to a $T^{3/2}$ power law expected for ferromagnetic magnons out of an ordered state.

The magnetic contribution to the heat capacity, ΔC , at low temperatures is obtained by subtracting the electronic (γT) and phonon (βT^3) contributions that dominate $C(T)$ in the range $10 < T < 24$ K. The plot of $\Delta C/T$ vs. T shown in Fig. 2b emphasizes the logarithmic behavior of $\Delta C/T$ for $B = 0$ and 1.1 T for $T < 10$ K. The strong enhancement of $\Delta C/T$ with only weak applied fields < 1.5 T reflects the growth of quantum critical fluctuations near a ferromagnetic instability. The strong competition between a ferromagnetic state and spin fluctuations can be inferred from the intermingling of the log T -dependence and the hump in $\Delta C/T$ located near 4.5 K, which, for $\mu_0 H = 3$ and 5 T, broadens as the low-temperature, singular behavior of $\Delta C/T$ disappears.

The detailed field dependence of C/T reveals two interesting features shown for representative isothermals in Fig. 2c. (1) C/T peaks at a critical field H_c that separates a regime for $H < H_c$ where $C/T \sim -\log(T)$ increases with H , from the complementary regime for $H > H_c$ where the $\log(T)$ dependence weakens and eventually disappears. The peak fades and C/T becomes much less field dependent for $T > 4$ K. On the basis of the $C(T,H)$ data an H - T phase diagram (Fig. 3a) can be constructed to reveal a linear increase of H_c

with temperature that can be extrapolated to $T = 0$ K to locate the QCP at $\mu_0 H_c = 0.23$ T.

(2) All C/T curves converge at $\mu_0 H = 3$ T (indicated by an arrow in Fig. 2c). This is unlikely to be a coincidence, as an applied field $\mu_0 H = 3$ T clearly renders C/T temperature independent (see Fig.2a), indicating a possible crossover to Fermi liquid behavior.

It is also worth mentioning that the Wilson ratio, $R_W \equiv 3\pi^2 k_B^2 \chi / \mu_B^2 \gamma$, is 74.96 at $T = 1.8$ K and shows weak temperature dependence below 4 K, as shown in Fig.3b. This strikingly large R_W is clearly the consequence of incipient ferromagnetism, and is far beyond the values (e.g., $R_W \sim 1-6$) typical of heavy Fermi liquids and exchange-enhanced paramagnets such as Pd [31]. But R_W drops rapidly at $T > 4$ K where the C/T peak fades (see Fig.3a), reaffirming the crossover to Fermi liquid behavior (see Fig.3b).

The presence of the quantum critical fluctuations is further corroborated by the temperature dependence of the **c**-axis ρ_c and **ab**-plane ρ_{ab} resistivities as a function of T , shown in Fig. 4a. The residual resistivity ρ_0 is $2.2 \mu\Omega \text{ cm}$ and $0.66 \text{ m}\Omega \text{ cm}$ for ρ_{ab} and ρ_c , respectively, and the residual resistance ratio $RRR \approx 3$. An interesting feature is that ρ_c and ρ_{ab} exhibit a $T^{3/2}$ law over a wide temperature range up to 120 K, which is particularly strong for ρ_c , as shown in Fig. 4b, where ρ_c vs T^2 (upper scale) is also shown for comparison. At $\mu_0 H \geq 5$ T, the temperature dependence of ρ changes from $T^{3/2}$ to T^2 (see inset), suggesting a recovery of Fermi liquid behavior. It is remarkable that ρ exhibits a large anisotropy ($\rho_c/\rho_{ab} \sim 300$) that is essentially temperature independent, implying quasi-two-dimensional transport, although the magnetic susceptibility is much less anisotropic, suggesting three-dimensional magnetic correlations. There are no

indications for long-range orbital order, possibly because the Ir-ions are on sites of low symmetry.

The $T^{3/2}$ and $T^{5/3}$ laws are seen in QCP systems such as MnSi [24], $\text{Sr}_3\text{Ru}_2\text{O}_7$ [2], $\text{Sr}_4\text{Ru}_3\text{O}_{10}$ [23, 32], and some heavy fermion systems [24]. The $T^{5/3}$ -dependence is attributed to dominant low-angle electron scattering by low- q spin fluctuations [24], hence weakening the temperature dependence of the resistivity from T^2 . The power-law $T^{3/2}$ is thought to be associated with effects of diffusive electron motion caused by strong interactions between itinerant electrons and critically damped very-long-wavelength magnons [19]. Electron scattering by static imperfections will render these modes inoperative and a T^2 -dependence expected in Fermi liquid theory will result. The presence of the $T^{3/2}$ behavior at low temperature is therefore another indication that the crystals studied are of high quality.

All results presented here coherently support a scenario that SrIrO_3 is quite close to a QCP and that the observed physical properties are overwhelmingly dominated by strong spin fluctuations. This first study on single-crystal SrIrO_3 reveals it to be a *stoichiometric oxide* with unusual sensitivity to low magnetic fields, which makes it an outstanding model system for studies of quantum criticality. Given the phase diagram of Fig. 3a and the association of weak ferromagnetism with triplet-paired superconductivity near a QCP, it is urgent to explore the physical properties of SrIrO_3 in the milli-Kelvin range and at high pressures.

Acknowledgement: G.C. would like to thank Dr. W. Crummett for useful discussions. This work was supported by NSF through grants DMR-0240813 and 0552267. P.S. is supported by the DOE through grant DE-FG02-98ER45707.

References

1. Y. Maeno, et al., H. Hashimoto, K. Yoshida, S. Nishizaki, T. Fujita, J.G. Bednorz, and Lichtenberg, *Nature* **372**, 532 (1994).
2. S.A. Grigera, R.P. Perry, A.J. Schofield, M. Chiao, S.R. Julian, G.G. Lonzarich, S.I. Ikeda, Y. Maeno, A.J. Millis and A.P. Mackenzie, *Science* **294**, 329 (2001).
3. T. Siegrist and B.L. Chamberland, *J. Less-Common Metals*. **170**, 93 (1991)
4. A. V. Powell and P. D. Battle, *J. Alloys and Compounds* **191**, 313 (1993)
5. R. Lindsay, W. Strange, B.L. Chamberland, R.O. Moyer, *Solid State Comm.* **86** 759 (1993)
6. G. Cao, J.E. Crow, R.P. Guertin, P. Henning, C.C. Homes, M. Strongin, D.N. Basov, and E. Lochner, *Solid State Comm.* **113**, 657 (2000)
7. G. Cao, S. Chikara, X.N. Lin, E. Elhami and V. Durairaj, *Phys. Rev. B* **69**, 174418 (2004)
8. M.K. Crawford, M.A. Subramanian, R.L. Harlow, J.A. Fernandez-Baca, Z.R. Wang, and D.C. Johnston, *Phys. Rev. B* **49**, 9198 (1994)
9. D.C. Johnston, T. Ami, F. Borsa, M.K. Crawford, J.A. Fernandez-Baca, K.H. Kim, R.L. Harlow, A.V. Mahajan, L.L. Miller, M.A. Subramanian, D.R. Torgeson, and Z.R. Wang, in *Spectroscopy of Mott Insulators and Correlated Metals*, Ed. by A. Fujimori and Y. Tokura (Springer, Berlin, 1995), p249.
10. Q. Huang, J. L. Soubeyroux, O. Chmaisssen, I. Natali Sora, A. Santoro, R. J. Cava, J.J. Krajewski, and W.F. Peck, Jr., *J. Solid State Chem.* **112**, 355 (1994)
11. R.J. Cava, B. Batlogg, and K. Kiyono, Takagi, J.J. Krajewski, W. F. Peck, Jr., L.W. Rupp, Jr., and C.H. Chen, *Phys. Rev. B* **49**, 11890 (1994)

12. G. Cao, J. Bolivar, S. McCall, J.E. Crow, and R.P. Guertin, Phys. Rev. B, **57**, R 11039 (1998)
13. S. J. Moon, M. W. Kim, K. W. Kim, Y. S. Lee, J.-Y. Kim, J.-H. Park, B. J. Kim, S.-J. Oh, S. Nakatsuji, Y. Maeno, I. Nagai, S. I. Ikeda, G. Cao, and T. W. Noh, Phys. Rev B **74**, 113104 (2006).
14. G. Cao, Y. Xin, C. S. Alexander, J.E. Crow and P. Schlottmann, Phys. Rev. B **66**, 214412 (2002).
15. Magnetism in spin chains with geometric frustration has been recently observed in insulating $\text{Ca}_5\text{Ir}_3\text{O}_{12}$ and Ca_4IrO_6 , for example, G. Cao, V. Durairaj, S. Chikara, S. Parkin and P. Schlottmann, Phys. Rev. B **75**, 134402 (2007).
16. L. E. De Long, J. G. Huber and K. S. Bedell, J. Magn. Magn. Mat. **99**, (1991).
17. G. Cao, S. McCall, J.E. Crow and R.P. Guertin, Phys. Rev. Lett. **78**, 1751 (1997).
18. X. N. Lin, Z.X. Zhou, V. Durairaj, P. Schlottmann and G. Cao, Phys. Rev. Lett. **95**, 017203 (2005).
19. C. Pfleiderer, M. Uhlarz, S.M. Hayden, R. Vollmer, H. von Lohneysen, N.R. Bernhoeft, and G.G. Lonzarich, Nature **412**, 58 (2001).
20. D. Aoki, A. Huxley, E. Ressouche, D. Braithwaite, J. Floquet, J.P. Brison, E. Lhotel, and C. Paulsen, Nature **413**, 613 (2001).
21. C. Pfleiderer, S.R. Julian, and G.G. Lonzarich, Nature **414**, 427 (2001).
22. G. Cao, S. Chikara, J. W. Brill, and P. Schlottmann, Phys. Rev. B **75**, 024429 (2007)
23. For example, G.R. Stewart, Rev. Mod. Phys. **73**, 797 (2001).
24. M. B. Maple, Physica B **215**, 110 (1995).

25. M. B. Maple, M. C. de Andrade, J. Herrmann, Y. Dalichaouch, D. A. Gajewski, C. L. Seaman, R. Chau, R. Movshovich, M. C. Aronson and R. Osborn, *J. Low Temp. Phys.* **99**, 223-249 (1995).
26. J.M. Longo, J.A. Kafalas, and R.J. Arnott, *J. Solid State Chem.* **3**, 174 (1971).
27. K. Yamaura and E. Takayama-Muromachi, *Phys. Rev. B* **64**, 224424 (2001).
28. D.J. Singh, *Phys. Rev. B* **67**, 054507 (2003).
29. B.T. Matthias and R.M. Bozorth, *Phys. Rev.* **109**, 604 (1958).
30. B.T. Matthias, A.M. Clogston, H.J. Willaims, E. Corenzwit, and R.C. Sherwood, *Phys. Rev. Lett.* **7**, 7 (1961).
31. L.E. DeLong, R.P. Guertin, S. Hasanain, and T. Fariss, *Phys. Rev. B* **31**, 7059 (1985).
32. S. Chikara, V. Durairaj, W.H. Song, Y.P. Sun, X.N. Lin, A. Douglass, G. Cao, and P. Schlottmann, *Phys. Rev. B*, **73**, 224420 (2006).

Captions:

Fig.1. (a) The magnetic susceptibility χ as a function of temperature at $\mu_0H= 0.5$ T for $H \parallel \mathbf{c}$ -axis (χ_c) and $H \perp \mathbf{c}$ -axis (χ_{ab}). χ for polycrystalline IrO_2 is also shown for comparison; Inset: Isothermal magnetization M vs. H at $T=1.7$ K; (b) Reciprocal susceptibility χ_c^{-1} and χ_{ab}^{-1} as a function of temperature for $\mu_0H= 0.5$ T; (c) χ_c^{-1} as a function of $T^{1/2}$ and T (upper scale, for $B=0.8$ T marked by an arrow). The behavior of χ_{ab}^{-1} is similar and not shown.

Fig.2. (a) The specific heat C divided by temperature, C/T , vs. $\log T$ for $\mu_0H=0, 0.5, 1.1, 3, 5,$ and 8 T; and C vs. $T^{3/2}$ (right and upper scales) for $\mu_0H= 8$ T. (b) $\Delta C/T$ vs. $\log T$ (see definition of ΔC in text) for $\mu_0H= 0, 1.1, 3, 5$ T; (c) C/T vs. H for some representative temperatures.

Fig.3. (a) An H - T phase diagram generated based on the data in Fig. 2. The dashed line is a guide to the eye; (b) The Wilson ratio R_W as a function of T . R_W is estimated based on χ and C/T at $\mu_0H=0.5$ T.

Fig.4. (a) The basal plane and c -axis resistivity, ρ_{ab} and ρ_c (right scale) as a function of temperature; (b) ρ_c vs. $T^{3/2}$ and T^2 (upper scale) for $1.7 < T < 120$ K at $\mu_0H=0$ T. Inset: ρ_c vs. T^2 for $1.7 < T < 37$ K at $\mu_0H=5$ T.

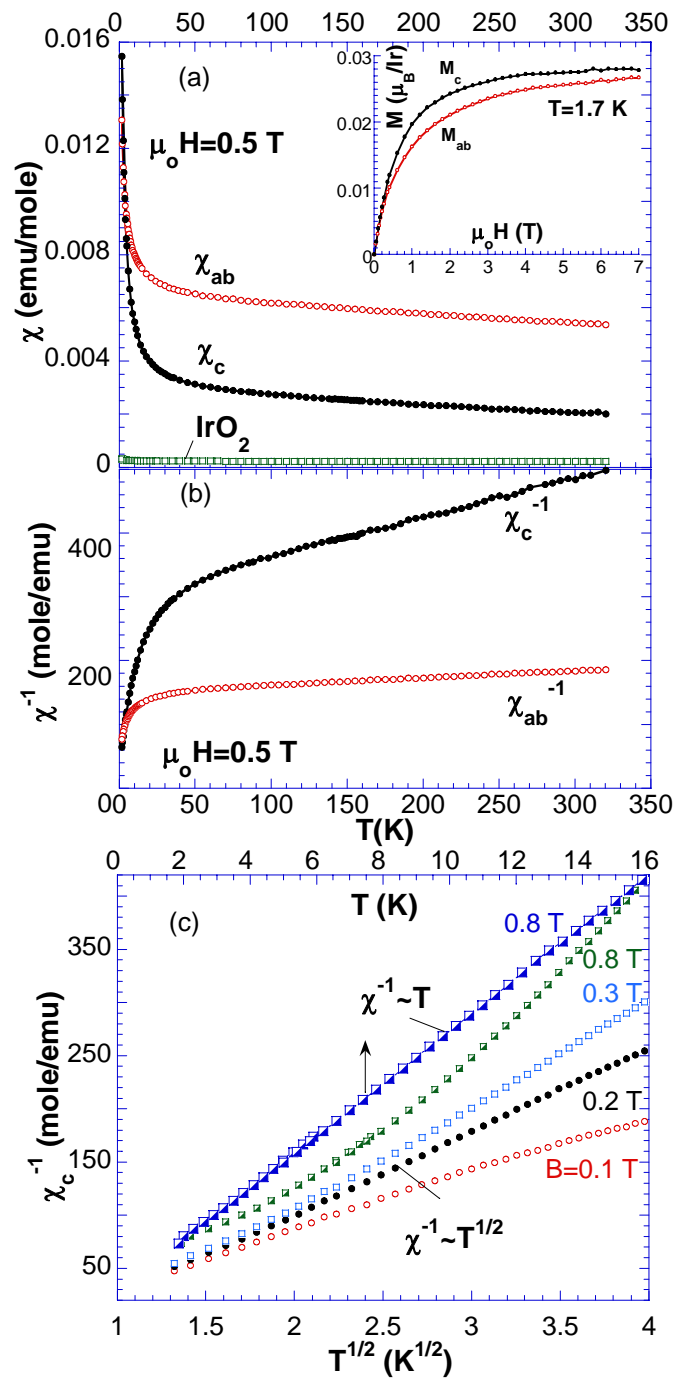


Fig. 1

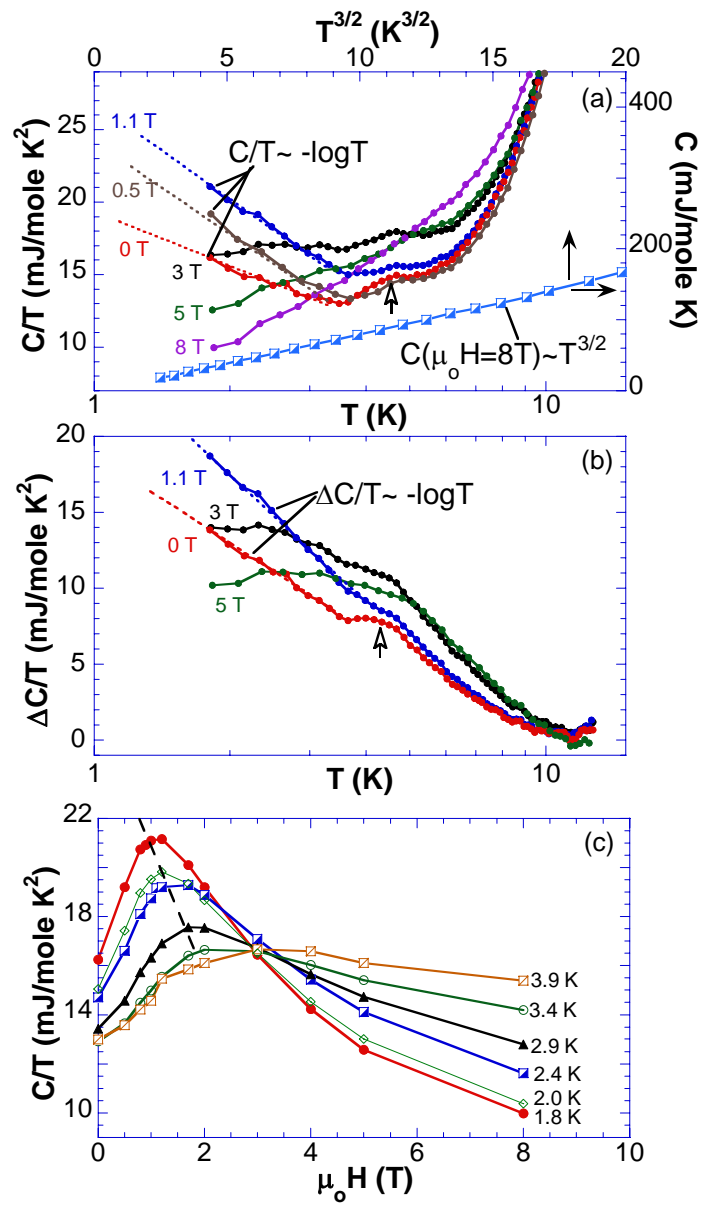


Fig. 2

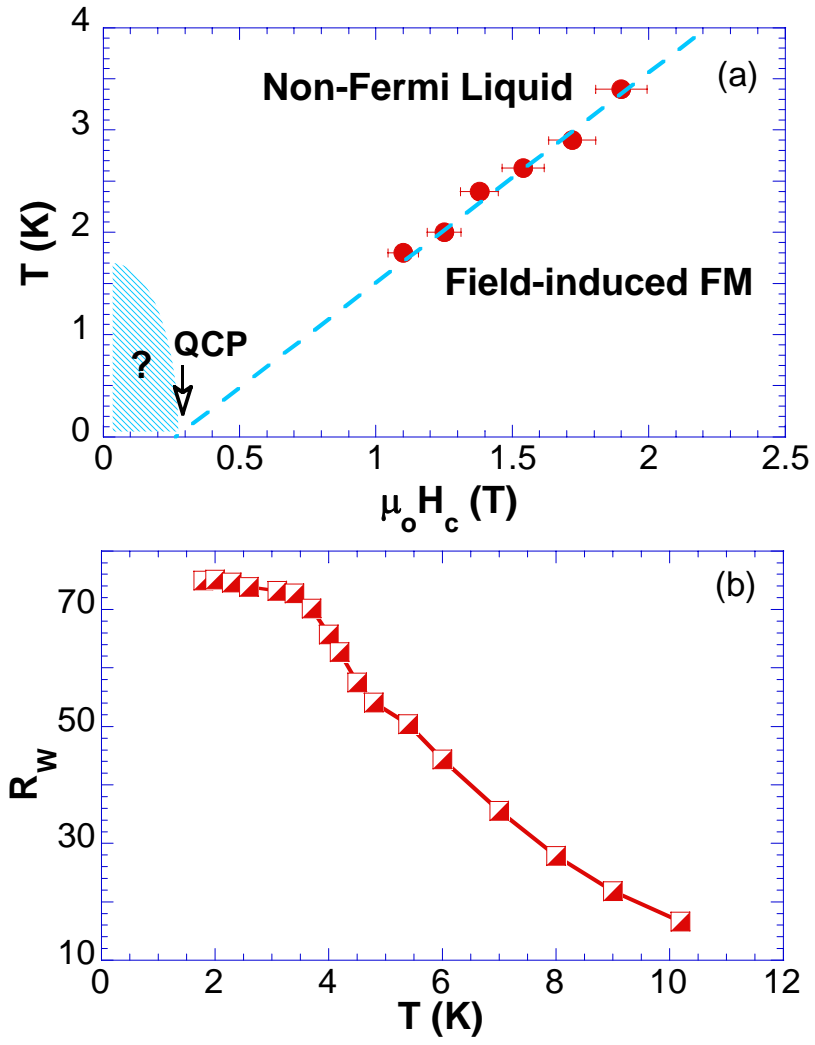


Fig. 3

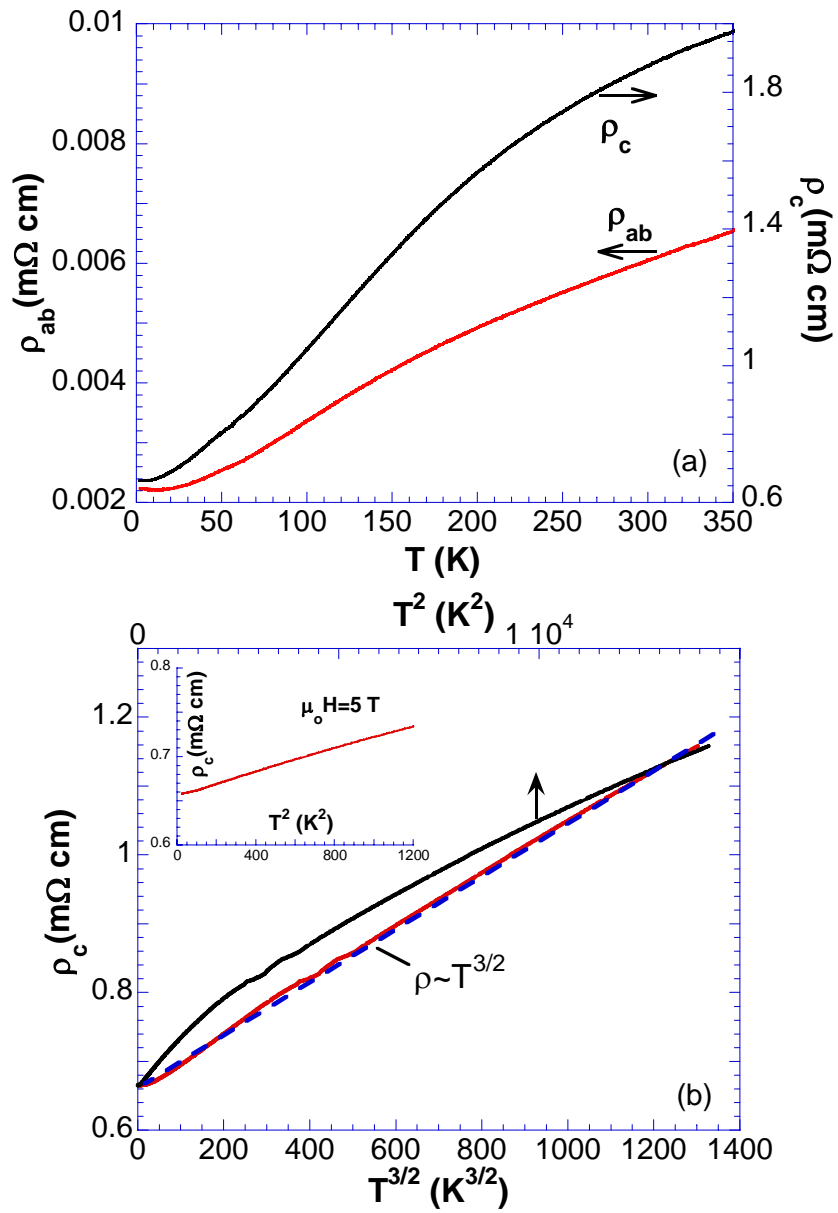


Fig. 4